MODERN ADVANCES IN OPTICAL MEASURING TECHNIQUES TOOLS TO SUPPORT ENERGY CONSERVATION

F. MAYINGER
Lehrstuhl A für Thermodynamik
Technische Universität München
Boltzmannstraße 15
D-85748 Garching

Abstract. Transport processes – heat and mass – play an important role in energy conservation. To optimise these processes, optical measuring techniques can be of great help. An overview is given on various optical measuring techniques, which give insight into transport processes, especially with heat transfer and with combustion. A short introduction into holography, holographic interferometry as well as Rayleigh Scattering and Laser Induced Fluorescence show, together with examples from several fields of thermo-fluiddynamic research work, the capabilities of optical measuring techniques to improve transport processes.

1. Introduction

As long as our energy demand is mostly provided via heat production, the optimisation of heat transfer plays an important role in energy conservation. Heat is generated by combustion processes to a large extent, and low combustion efficiency, with non-negligible content of partially unburned components in the exhaust gas, has a strong negative effect on energy conservation.

In heat recovery, the optimum design of heat exchanging components with respect to augmenting heat transport and minimising pressure drop plays an important role. Holographic interferometry provides detailed insight into the local conditions of the boundary layer in which heat transfer and friction are controlled. So these optical measuring techniques allow a well aimed strategy for improving heat exchanger performance.

The turbulent transport of mass and heat in and in front of the flame has a strong influence on the combustion process, and if both are too weak or if one prevails over the other, incomplete combustion is the consequence. Optical techniques, like Raman Scattering, Laser Induced Fluorescence or Auto Fluorescence allow us to follow the combustion process in detail and give precise and instantaneous information about the flame structure. These optical techniques do not only monitor the combustion process itself; they also give very valuable hints to how and where to influence the process in a posi-

S. Kakaç et al. (eds.), Heat Transfer Enhancement of Heat Exchangers, 357–379.

tive way to achieve high combustion efficiency and low content of toxic components in the exhaust gas.

If liquid fuel is used for combustion processes, adequate spray-formation is the key for efficient burning of the flame. Droplet distribution and droplet movement in the spray can be conveniently monitored and measured by holography especially by double-pulse holography.

During the last 5 or 10 years, the development of optical methods has been supported by the availability of new equipment like high energy light sources, intensified electronic camera systems and electronic devices as well as new software for image evaluation. This allows us to reduce the time of data processing, which has been very time consuming in the past.

measuring technique	physical effect	application	dimensions	real-time application
schlieren and shadow	light refraction	heat, mass transfer	2D (integ)	yes
holography	holography	particle size, velocity	3D	no
interferometry	change of light velocity	heat, mass transfer	2D (integ)	yes
laser Doppler velocimetry	Mie scattering	flow velocity	point	yes
Raman scattering	Rayleigh scattering	density, temperature	point-2D	yes
dynamic light scattering	Raman scattering	mol. concentration, temperature	point-1D	no
laser induced fluorescence	fluorescence	concentration, temperature	point-2D	no
absorption	absorption	concentration, temperature	point-2D (integ.)	yes
pyrometry	thermal radiation	temperature	1D	yes
thermography	thermal radiation	temperature	2D (integ)	yes
self fluorescence	therm. fluorescence, chemoluminiscence	concentration, temperature	2D (integ)	yes

TABLE 1. Over-view of optical measuring techniques

It is well known that optical methods work in a non-invasive and inertialess way, and therefore do not influence the thermo-fluiddynamic process that has to be investigated.

In principle, one can distinguish between imaging and non-imaging techniques. Imaging techniques provide simultaneous information on a large area, and use any kind of conventional or electronic means to store this information. Non-imaging optical methods are of local nature, i.e., they work with focussed light beams (mostly laser) and usually register data of a very small volume, usually smaller than 1 cubic-millimeter. Table 1 presents a list of examples for modern optical measuring techniques used in fluiddynamic processes and in combustion. This table also gives information about the physical effect used in the various techniques, and presents examples for application. As

it is not possible to discuss all the optical techniques, known from the literature, in detail here, emphasis is given to

- Holography,
- Holographic Interferometry,
- Raman Scattering,
- Laser Induced Fluorescence (LIF, LIPF) and
- Auto Fluorescence.

A detailed overview over several optical measuring techniques, their working principle and their application is given in [1].

The evaluation of optical data, for example, from a hologram, from an interferogram, from Raman Spectroscopy, or from Laser Induced Fluorescence, has become much faster in the last years than it could be done in the past. A few years ago it took hours to evaluate an interferogram. Today the same work is done by a computer within a few seconds. But also the huge storage capacity of modern computers – even of the PC type – was an important requirement for preparing the way for the revival of optical methods.

2. Holography

In the middle of this century Gabor [2] invented a new method for recording and storing optical information, which was called holography. Unlike photography, which can only record the two-dimensional distribution of the radiation emitted by an object, holography can store and reconstruct three-dimensional pictures. The name holography comes from the ability of the method to record the totality (holos) of the light information, respectively, of the wave front, namely the amplitude (as brightness), the wave-lengths (as colour) and the phase position of the light. By using these possibilities, completely new interference methods can be developed. Holography, however, demands a source emitting coherent light. Therefore, holography, as invented by Gabor in 1949, could only be widely used when the laser was developed, which was 10 years later.

The general theory of holography is very comprehensive and the interested reader is referred to the literature [3, 4, 5]. Here only a set-up for monitoring spray systems will be briefly explained. To create a hologram of any object, this object has to be illuminated by a monochromatic light source, usually a laser. The reflected or scattered light (object wave) has a very complicated wave form. According to the principles of Huygens, one can regard it as the superposition of many elementary spherical waves. Fig. 1 shows the optical arrangement for so-called "through-light" holograms, consisting of illuminating lasers, various lenses and mirrors. The object wave in this arrangement is produced by a pulsed ruby laser, and this object wave travels via a diverging lens, a beam splitter and a ground glass through the spray (measured object) onto a photographic plate, called in this case hologram. In the beam splitter, part of the laser beam is deflected, bypasses the measured object and falls also onto the hologram. This wave is called reference wave. The superposition of the object wave and the reference wave

produces an extremely fine (microscopic) fringe pattern on the photographic plate, the hologram.

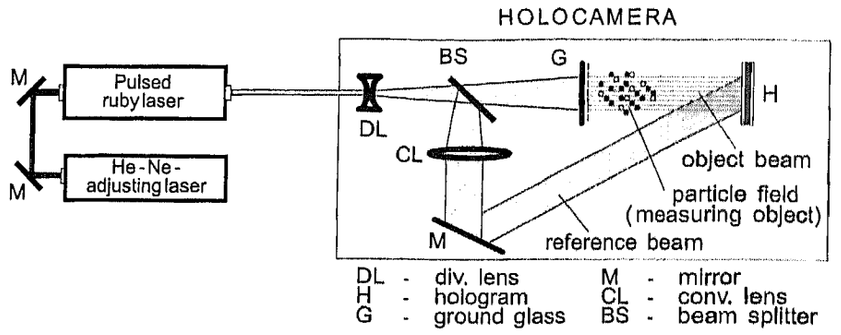

Figure 1. Holographic set-up for through-light, ultra-short time exposures with a pulsed laser

The pulsed ruby laser produces an ultra-short monochromatic light flash of 30 ns duration and a wave-length of 693 nm. The helium-neon laser, also shown in Fig. 1, is only used for adjusting the optical arrangement. The helium-neon laser produces continuous red light of similar wave-length as the ruby laser. The ruby-rod is transparent for the light of the helium-neon laser, so the adjusting light is exactly in line with the recording light.

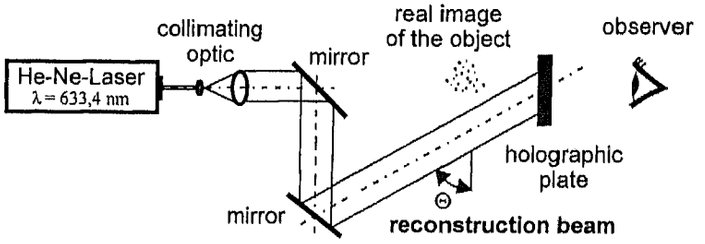

Figure 2. Optical arrangement for the reconstruction of pulsed laser holograms

After the illumination, the photographic plate is chemically processed - developed, fixed and dried - and it is then repositioned into the light-beam of the helium-neon laser, as shown in Fig. 2. However, it is illuminated only with the reference wave, which is called reconstruction wave now. This illumination by the reconstruction wave produces two images of the former measured object - the spray - a virtual image and a real one. These images appear on different sides of the hologram. The virtual image can be observed with the naked eye, and it provides, to a certain extent, a three-dimensional information of the droplet distribution in the spray. The real image - see Fig. 3 - can be looked at by using a microscope or also any camera, for example a video camera. This real image has a three-dimensional extension, and by using a very long focus lens for the camera, only one plane in the real image of the spray will be recorded sharply. If we now place our video camera on a traversing mechanism (Fig. 3), we can take two-dimensional pictures of several planes of the measured object by moving the video camera forward and backward, and so we can store the three-dimensional information in

a computer. One can argue that this recording, plane by plane, could also be done by changing the focal length of the lens in the camera. In this case, however, we would get different reproduction scales for the planes.

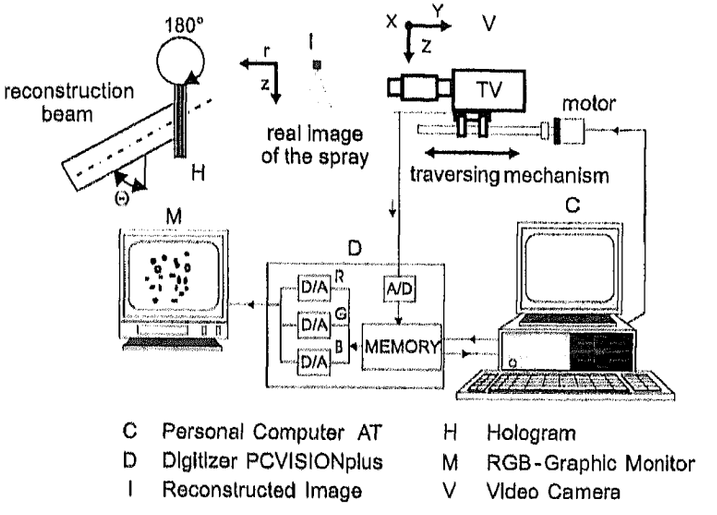

Figure 3. Digital Image-Processing System for the evaluation of pulsed laser holograms

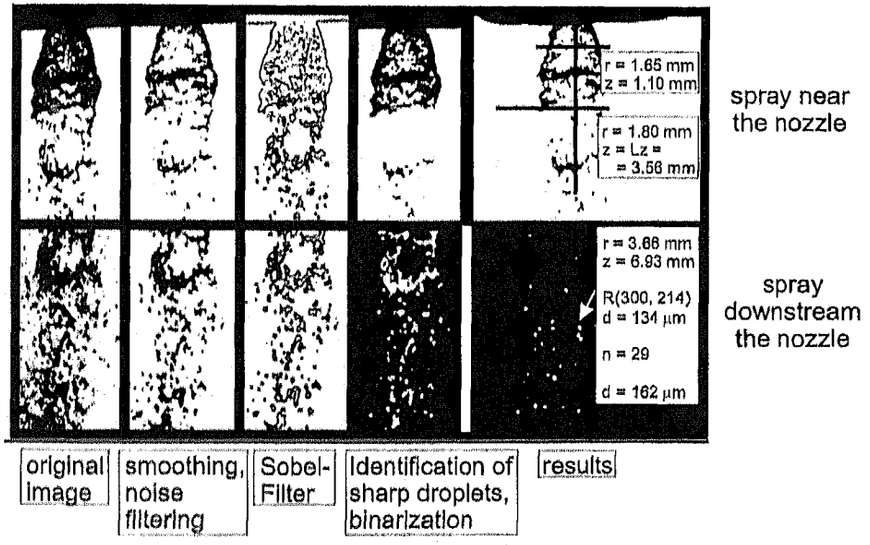

Figure 4. Steps of Image-Processing of a hologram
Upper row: spray near the nozzle
Lower row: spray downstream of the nozzle

The digital image processing system, together with the camera monitoring the real image, coming out from the hologram via the reference wave, is also shown in Fig. 3. The data from the video camera - a CCD camera - are given to a digitiser and are reprocessed in a personal computer. In the computer a complicated image evaluating process is performed. Fig. 4 gives a visual impression of how the numerical procedure, going on in the computer, changes the original photographic picture into a computerised one.

A spray veil and a swarm of particles with different grey values in the range from black to white (via grey) representing droplets of this spray and a pattern of fine grain, which formed the optical noise (speckle noise), is seen in the first scene (left) in Fig. 4. This disturbing noise is produced by the diffusive monochromatic illumination necessary for recording the hologram. This noise at first is removed in the computer by a so-called noise filter (second scene from left). After the separation of the droplet images from the background, the identification of sharply focussed droplets, the measurement of their projected areas, and the evaluation of their equivalent diameters and centre-points can be performed (third and fourth scene in Fig. 4). An important step within this procedure is to eliminate all optical reproductions of droplets which are out of the focus plane. This is done by determining the gradient of greyness at the boundary of the reproduction of the droplet. Those droplets which are in the focus plane have a large gradient of greyness. For a detailed description of this image processing, reference is made to [1 (chapter 7)].

Finally, the computer reproduces the image of one single plane out of the spray, as shown in the right scene of Fig. 4. In this example the focussed plane represents a slice out of the spray, thinner than 0,5 mm.

From this figure one can now derive the length of the liquid veil, until it disrupts in droplets, and the thickness of its liquid layer. It can be clearly seen, that the veil has a wavy form and its liquid flow is characterised by a week pulsation with an oscillatory production of more or less dense droplet clouds. Far downstream of the veil one can identify the droplets with respect to their diameter and their concentration in the cloud.

To get information about the velocity of the droplets we produce the so-called double-pulse holograms. To do this, one illuminates the photographic emulsion of the holographic plate twice before processing it. This can be done for example with a ruby laser, which allows the emission of more than one laser pulse within a short period of time (usually 1 - 800 µs). For slow-moving particles one can use an argon-laser emitting continuous light which, however, is periodically interrupted via a mechanical device or an optic chopper. The evaluation of such a double-pulse hologram is - as it is easily understandable - even much more complicated than that of a single-pulse hologram. At first, the procedure is the same as sketched out above. Then the computer produces connecting lines between each pair of optically reproduced droplets, without regarding whether it is the reproduction of the first or of the second illumination. The distance and the orientation (angle) of each connecting line are then calculated and stored in the computer. With the help of a Fourier-analysis, the normalised frequency of the angle and of the distance is then plotted versus the angle and the distance of the reproductions. If the flow in this spray is not too chaotic, two maxima are found, one for the angle and the other one for the distance. Both maxima can be used as average values for the spray angle and for the droplet velocity, because this average velocity can be easily calculated

by dividing the mean distance by the delay time between the first and the second illumination.

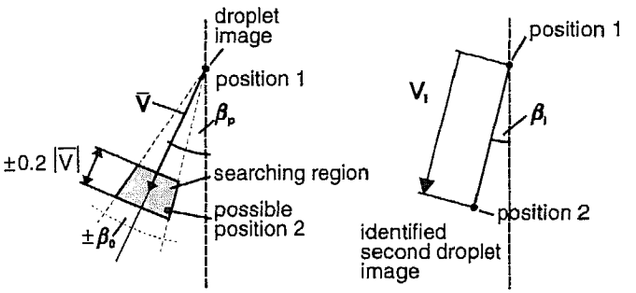

Figure 5. Method for evaluating single particle velocity from double-pulse holograms

One can now proceed one step further to calculate the real velocity of each single droplet. For this purpose one defines a searching area, as briefly lined out in Fig. 5. The centre of this searching area is given by the average values for the velocity and the angle of the droplets, and the extension of this area depends on the droplet concentration on the spray, because there should be only one optical reproduction of a droplet in this area. Therefore, for very dense sprays or particle clouds this procedure has some limitations.

In total, this holographic velocimetry gives reasonable results, as Fig. 6 proves. In this figure the average droplet velocity of a spray is plotted versus the mass flow rate with the pressure of the spray atmosphere as the parameter. The measuring technique clearly records the influence of the spray atmosphere and presents a reduction of the droplet velocity with increasing the air density, due to a higher pressure.

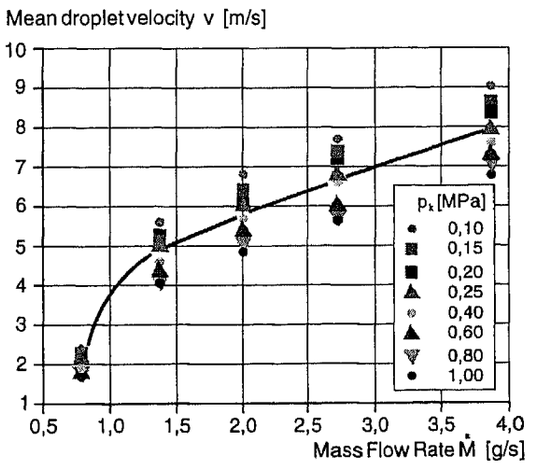

Figure 6. Mean droplet velocity in a spray as a function of the flow rate at different ambient pressures

Of course similar results can also be gained by Particle-Image Velocimetry (PIV) in which a thin light sheet, produced by cylindrical lenses, penetrates the droplet cloud, illuminating the particles there. The particles which are momentarily present in this light sheet can be recorded with a normal high-speed camera. In this case, however, only the velocity parallel to the light sheet can be determined. Particles moving orthogonal to the light sheet cannot be followed up. With the double-pulse holography these particles can be found by evaluating adjacent planes successively after the treatment of the first plane. The procedure is mathematically complicated. A brief description can be found in [6, 7].

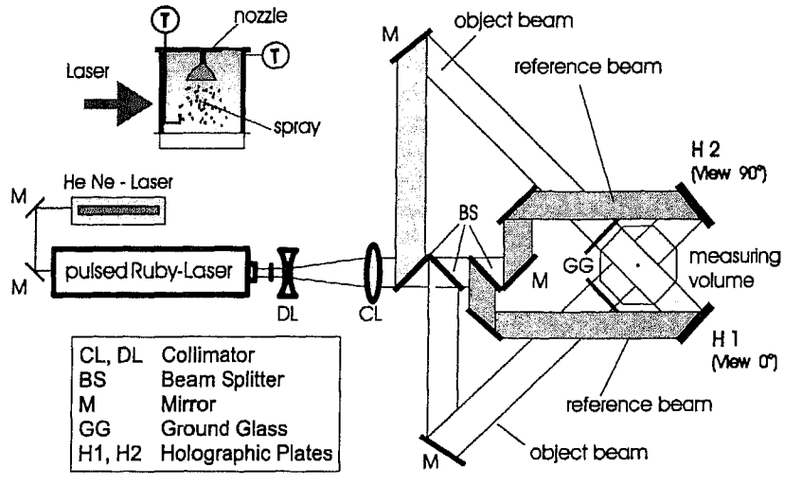

Figure 7. Holographic set-up for stereo-matching of strongly three-dimensional measurement problems The two holographic plates are exposed at the same time

For a real stereo matching of strongly three-dimensional measurement problems a holographic set-up can be used, as shown in Fig. 7. Two holograms are recorded simultaneously perpendicular to each other. Both holograms have to be scanned and digitised by a camera, which is again focussed stepwise along the depth coordinate in order to record the entire three-dimensional information contained in the holographic images. The procedures for evaluating these images and for reprocessing the data are briefly described in [8]. This optical set-up and its data processing can be used for investigating three-dimensional bubble flow, for example in stirrers.

3. Holographic Interferometry

By using the recording capabilities of holography, different waves - even those shifted in time - can be stored in the same holographic plate, as we learned when discussing double-pulse holography in chapter 2. If the developed holographic plate is illuminated with the reference wave, all object waves are reconstructed simultaneously. Where they differ only slightly from each other, interference patterns are observed. These are the fundamentals of holographic interferometry.

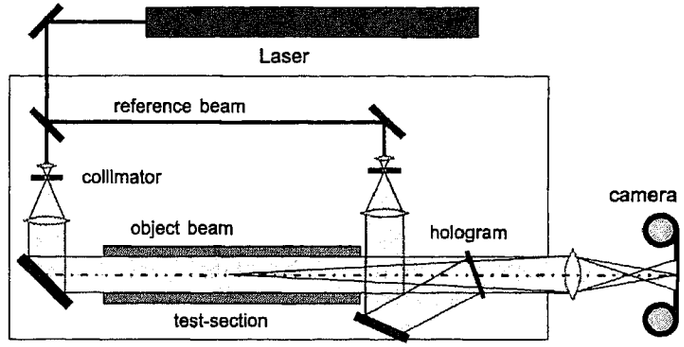

Figure 8. Optical set-up for holographic interferometry

In heat and mass transfer the temperature and the concentration distribution in a fluid are of special interest. To investigate processes with heat or mass transfer a so-called through-light method is used, where the object wave is irradiating through a volume in which the transport processes take place. A simple exemplary arrangement for holographic investigations is shown in Fig. 8. A beam splitter divides the laser-beam into an object wave and into a reference wave, which is also called comparison wave. Both waves are expanded to parallel wave bundles behind the beam splitter via lenses, usually consisting of an arrangement of a microscopic lens and a collecting lens. The expanded and in a parallel way organised object wave travels through the space of the research object of interest - the test section - in which the distribution of temperature or concentration is studied. The reference wave bypasses the test section and falls directly onto the photographic plate.

The benefit of holographic interferometry compared to other interferometric methods - like Mach-Zehnder Interferometry - is that there is no need for a high optical quality of the optical components, because only relative changes of the object wave are recorded, and optical errors are automatically compensated in this interferometric method. On the other hand, the monochromatic light producing the wave front has to be very stable, therefore a laser of good coherency is needed as a light source. For more details on holographic interferometry reference is made to the literature [1, 9, 10].

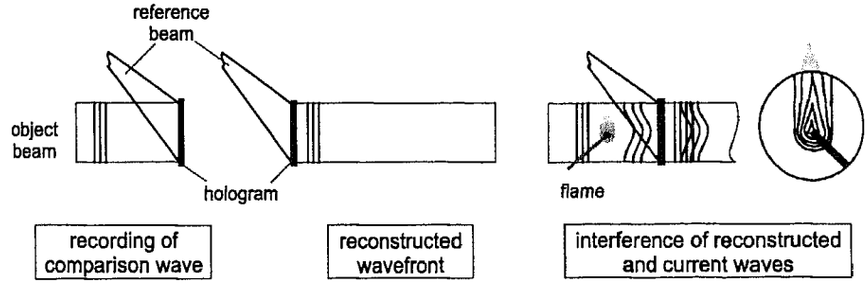

Figure 9. Real-time method for holographic interferometry

Several procedures exist to produce interferograms. Here, only the so-called "real-time method" will be explained, which can also be used in connection with high-speed cinematography. This method observes the process to be investigated in real-time and continuously. The method is illustrated in Fig. 9. After the first exposure by which the comparison wave is recorded and during which no heat transfer is going on in the test section, the hologram is developed and fixed. Afterwards, accurately repositioned, the comparison wave is reconstructed continuously by illuminating the hologram with the reference wave. This reconstructed wave showing the situation without heat transfer in the test section can now be superimposed onto the momentary object wave. If the object wave is not changed, compared to the situation before the chemical developing process, and if the hologram is precisely repositioned, no interference fringes will be seen on the hologram. This feature is a valuable help to replace the hologram accurately.

Now the heat transfer process can be started. Due to the heat transport, a temperature field is formed in the fluid and the object wave receives an additional phase shift when passing through this temperature field. Behind the hologram, both waves interfere with each other and the changes of the interference pattern can be continuously observed or photographed.

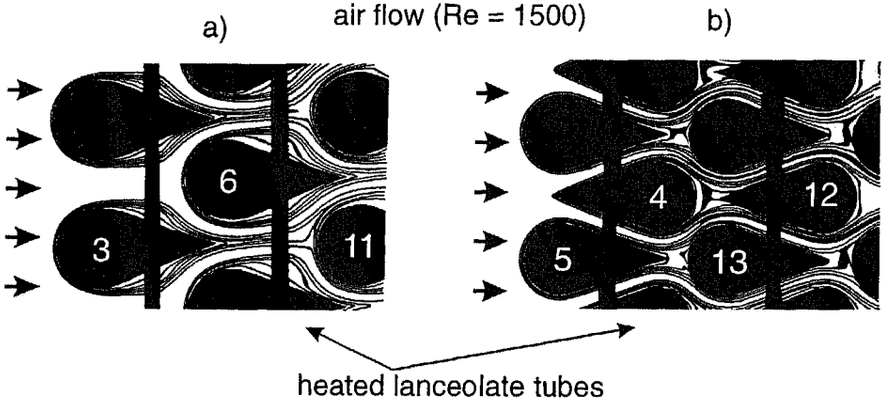

Figure 10. Interferograms of cross-flow through bundles of lanceolate tubes
a) uniformly orientated; b) mixed orientation (even rows reversed)

It has to be mentioned that interference fringes are created by density gradients and these can originate from temperature-, pressure- or concentration-differences. In a single component fluid with flow velocities far away from the sound velocity, interference fringes are only the product of temperature differences, and each line - black or white - represents - in a first approximation - an isotherm in the fluid. When the isotherms are densely packed, there are steep temperature gradients and therefore a high local heat transport. For the evaluation of such interferograms, reference is made to [1 and 10]. Examples of holographic interferograms, taken with the real-time method, are illustrated in Fig. 10.

The task of the research project, in which the interferograms in Fig. 10 were produced, was to develop a compact heat exchanger operating at very low air pressure (cross-flow) with a good overall performance, i.e., maximum total heat flux and low

friction. One has to be reminded that the total heat flux is the product of the average heat transfer coefficient and the heat transferring surface to the ambient air. The low ambient pressure resulted in low Reynolds numbers.

Tubes of lanceolate cross-section can be much more densely packed than tubes of circular cross-section. They also have a lower pressure drop at the same air flow rate. The most dense package can be achieved if every second row of the bundle has reversed orientation, as shown in Fig. 10b. This arrangement has a high density of heat transferring surface per volume of the heat exchanger. The question is what happens to the heat transfer coefficient or to the Nusselt number, if we reverse the orientation of the tubes in the even rows with respect to the odd ones.

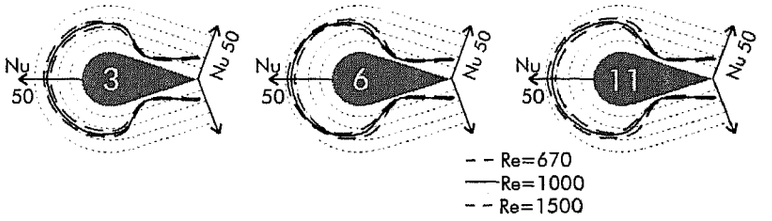

Figure 11. Evaluation of interferograms in Figure 10a, local Nusselt numbers around lanceolate tubes in bundle (positions see Figure 10a)

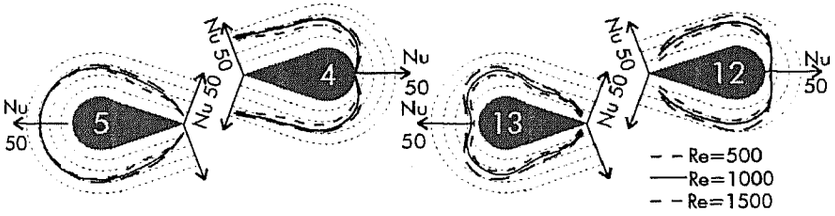

Figure 12. Evaluation of interferograms in Figure 10b, local Nusselt numbers around lanceolate tubes in bundle (even rows reversed, positions see Figure 10b)

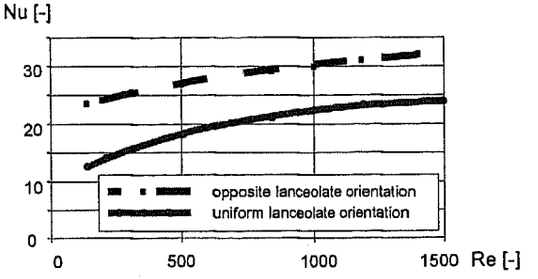

Figure 13. Average Nusselt numbers in cross-flow bundles with lanceolate tubes

From the interferograms in Fig. 10, reliable and accurate local Nusselt numbers can be evaluated around the lanceolate tubes, as shown in Fig. 11 and Fig 12. If all the tubes have the same orientation in the bundle, the position does not have too much influence on the Nusselt number, as Fig. 11 demonstrates. There the local Nusselt number versus

the circumference of the tubes in the rows 1, 2 and 3 (positions 3, 6, 11 in Fig. 10a) are plotted. One can clearly see that only two third of the surface of each tube participates in the heat transport.

If we turn the orientation of the tubes in every second row (even rows, positions 4, 5, 12, 13 in Fig. 10b), then the situation changes remarkably. As Fig. 12 demonstrates, the lanceolate tubes now have a much better heat transfer performance. This is clearly expressed, if we plot the average Nusselt numbers (averaged over the whole heat transfer area of the bundle) versus the Reynolds number, as done in Fig. 13. The improvement due to the reversed orientation of the tubes holds for a wide range of Reynolds numbers. As it is easily understandable, it is a little larger at very low Reynolds numbers than at higher ones. Therefore the reversed orientation of the tubes does not only allow a more compact design, it also improves the heat transfer performance.

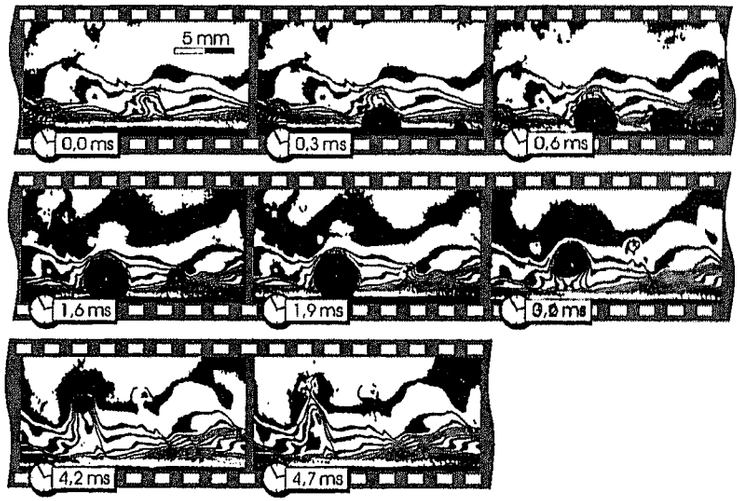

Figure 14. Holographic interferograms of the detachment and re-condensation of bubbles from a heated wall in sub-cooled water

With the simple holographic arrangement, shown in Fig. 8, not only can the heat transfer coefficients in a single-phase flow be measured; it can also be used for studying phenomena with phase change, for example with boiling. Fig. 14 shows a sequence of interferograms which were taken within a period of less than 5 µs in a horizontal water flow. The bulk temperature of the water flowing from right to left was slightly sub-cooled and the lower wall of the channel was heated to such an extent, that in spite of the fact that the bulk temperature was below the saturation temperature, sub-cooled boiling occurred at the wall.

If we look at the wall-near boundary layer we can detect that there is one area where a plume of hot liquid is a little more extended into the bulk region. In the period between 0,0 and 0,3 ms, a bubble is created and grows from the wall into this hot liquid plume. When the bubble penetrates the plume boundary, it comes into contact with the sub-cooled bulk and starts to condense (sequences from 1,9 to 4,7 ms) again. The whole span of life-time of this bubble is approximately 4,5 ms.

We can observe a second bubble which starts growing at a position of the wall where the boundary layer has a very steep temperature gradient (see right side of scene 0,3 ms). Apparently, the liquid adjacent to the wall at this position is much hotter than at the position of the first bubble, and therefore this second bubble grows much faster. However, it reaches the sub-cooled bulk earlier, which results in a very rapid condensation, and the life-time of this bubble is only in the order of 2 ms.

So holographic interferometry, together with high-speed cinematography, gives a very good insight into the phenomena of boiling and demonstrates that bubble growth and bubble condensation are not only governed by determining parameters, such as the heat flux or the sub-cooling, but has a stochastic nature, too. This stochastic nature originates from fluctuations in the temperature gradients of the boundary layer and its thickness. These fluctuations are influenced by the turbulence and also by the "history" of the bubble detachment.

From the interferograms in Fig. 14 we can also learn a limiting phenomena of this method. The laser light travelling through the fluid is not only shifted in phase, but it is also deflected by the density gradients. This light deflection is the reason why in Fig. 14 we do not get any information in the immediate neighbourhood of the heated wall.

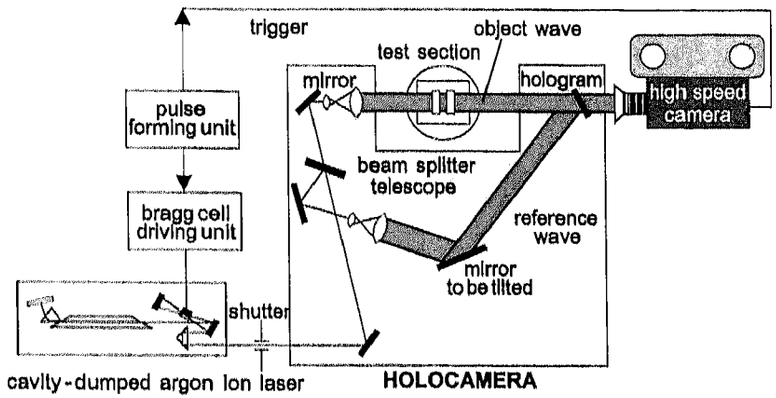

Figure 15. Arrangement of holographic interferometry with finite-fringe method

With very high heat transfer coefficients, the boundary layer at a heat transferring surface becomes very thin down to a few hundredths of a millimetre. In this case, it is difficult to evaluate the interference pattern, if it is registered with the procedure described up to now. A slightly altered method, the so-called "finite-fringe method" offers some benefits. In this method, after the reference hologram has been produced, a pattern of parallel interference fringes is created by tilting the mirror in the reference wave of Fig. 15 or by moving the holographic plate there within a few wave-lengths. The direction of the pattern can be selected as one likes, and it only depends on the direction of the movement of the mirror or of the holographic plate. This pattern of parallel interference fringes is then distorted by the temperature field due to the heat transport process. The distortion or deflection of each fringe from its original parallel direction is a measure for the temperature gradient at this spot and allows one to deduce the heat flux and therefore the heat transfer coefficient [11].

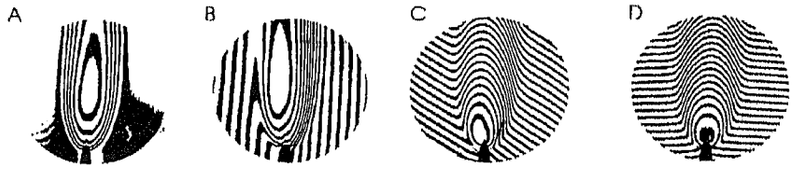

Figure 16. Comparison of an Infinite-Fringe-and a Finite-Fringe-Interferogram (various inclination angles of the mirror to be titled)

An example of how these "finite-fringe interferograms" differ from the method described before – infinite-fringe interferograms - is shown in Fig. 16. On the left upper side of Fig. 16 an infinite-fringe interferogram of the temperature distribution in a small gas flame is shown. All fringes represent lines of constant temperature, and as to be expected, the highest temperature is recorded in the centre line of the flame. The other 3 interferograms of this figure show finite-fringe interferograms of the same flame. These fringes do not represent lines of constant temperature, but the deviation of the fringes from their original direction (vertical, inclined or horizontal) gives the local temperature gradient in the flame. From this local temperature gradient it is easy to calculate the heat transport.

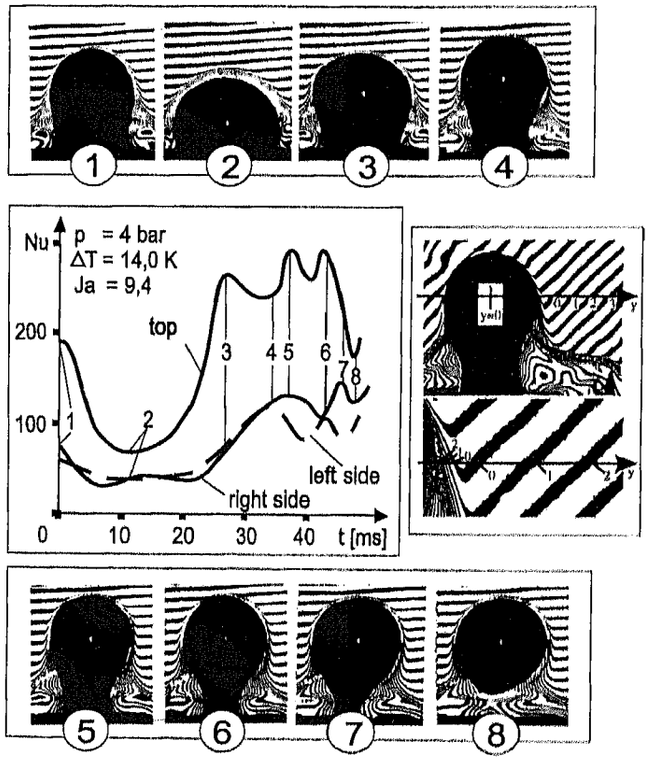

Figure 17. Heat transfer at the phase-interface of a steam bubble, condensing in sub-cooled water, deduced from a sequence of interferograms

Fig. 17 demonstrates an example for using these techniques in a flow with a bubble condensing in a liquid. The combination of this method with high-speed cinematography allows an inertialess and precise calculation of the heat transfer coefficient at the phase-interface of the condensing bubble. Steam is flowing out of a thin capillary against a slow downward water flow with a temperature, which is 14 K below the saturation temperature of the steam. With the penetration of the steam into the water the condensation starts, and after a few ms the reduction of the bubble volume by condensation is larger than the volumetric flow rate of the steam fed through the capillary. The bubble stops growing and a thin layer of saturated liquid is formed around its surface. This results in a sudden reduction of the heat transfer through the phase interface until the steam flow through the capillary can overcome the condensation rate again. The heat transfer increases and continues for a while with an oscillating character [11].

So holographic high-speed interferometry allows insights into thermo- and fluiddynamic phenomena, which could never be gained by conventional measuring techniques.

4. Light Scattering Methods

Light as a sensor can provide several information, and not only can the refractive index and the phase-shift be used to get information about the distribution of concentration or temperature in a substance. Besides the phase-shift, the effect of scattering is most commonly used to get information about the chemical and physical conditions in a gas or a liquid. Raman Scattering is a method which allows to measure the variety of substances present in a mixture, the concentration of each species and, under certain circumstances, also the temperature. Rayleigh Scattering can be used as a non-intrusive method for measuring the temperature. The fluorescence indicates the kind and the concentration of atoms and molecules and also allows me to deduce the temperature. There are also other scattering methods like Mie-Scattering used in Phase-Doppler-Velocimetry, Bragg-Scattering for detecting density fluctuations and for investigating the structure of crystals and finally also sound absorption. Here only the fluorescence used together with a light sheet method and Raman Scattering will be discussed.

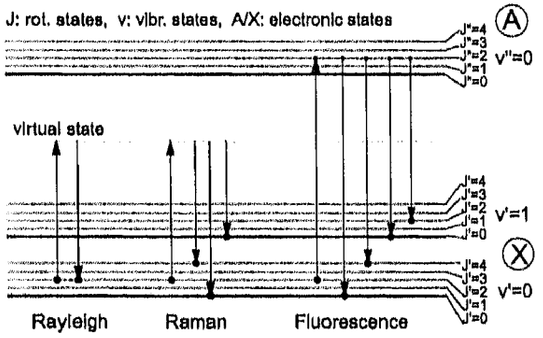

Figure 18. Energy diagrams for Rayleigh, vibrational Raman Scattering and Laser Induced Fluorescence

It should be briefly mentioned, that Mie-Scattering has been recently used for flow visualisation in Particle-Image Velocimetry (PIV). A laser-beam is formed into a very thin light sheet, illuminating a plane within the volume of interest. For one measurement two consecutive laser pulses are fired within a very short time interval, and the radiation scattered by the particles in the illuminated area is recorded by means of a two-dimensional camera. The diameter of scattering particles is usually between 3 μ and 300 μm.

If the particles, scattering the light, are smaller than the wave-length of the light, Rayleigh Scattering occurs. Typical scattering particles in this case are molecules. There are two models to describe the interaction between the incoming light and the molecule, namely the model of oscillating dipoles and the simplified quantum mechanical model. For details, reference is made to Bohren and Huffman [12].

In Raman Spectroscopy a molecule initially absorbs a photon of the light hitting it. For visible light the energy of this photon is higher than what can be stored by rotation or vibration in the molecule, but often lower than the difference between the ground level and the first electronic state of the photon. Therefore the molecule is lifted up to a highly unstable virtual level by absorbing the photon for a moment. The molecule afterwards immediately drops back to a stable energy level by emitting a photon. If this new level is identical with the original level, Rayleigh Scattering will be observed. The principle of this change in energy is shown in Fig. 18. If the new level is lower than the original level the scattered light has a different frequency than the incidenting light. The shift in frequency is referred to as the Raman Shift and it is proportional to the energy difference between the two molecular levels involved. One has to distinguish between rotational levels and vibrational levels of the molecule, and the difference between two rotational levels is much smaller than that of two vibrational levels. In Fig. 18 the change in energy is shown for Rayleigh Scattering, for Raman Scattering and also for Laser Induced Fluorescence within 2 vibrational levels.

Since every species has its own energetic structure, the observed frequency shift can be related to certain molecules. Raman Scattering therefore provides an excellent possibility for detecting the concentration of several species in a gas mixture of interest.

With Laser Induced Fluorescence the molecule under consideration also absorbs one photon of the incoming laser light. In this case, however, the energy of the photon must be equal to the energetic difference of two energy levels, the original level in the ground electronic state and the corresponding level in the first electronic state (see Fig. 18).

4.1 RAMAN SPECTROSCOPY

The theory of Raman Spectroscopy is well described in the literature [13, 14, 15]. Raman Spectroscopy is applicable to any transparent medium regardless of its physical state. In heat and mass transfer the applications are usually concentrated to liquid or gaseous states while chemical and biological applications of it deal with solid samples.

Based on the Raman effect various methods for the measurement of temperature and concentration have been developed, and some of them rely on special molecular resonance effects. The most widely used methods are Spontaneous Raman Scattering (SRS) or the Coherent Anti-Stokes Raman Scattering (CARS). The latter one provides light signals of higher intensity, which is especially useful for gaseous applications. On the other hand the set-up and the evaluation of the results are much more complicated for CARS than for SRS.

An example for a set-up to measure species concentration and temperature with Raman Spectroscopy is shown in Fig. 19. Raman Spectroscopy is a spot-wise measuring technique and the laser beam is therefore focussed on a small spot, of which the diameter forms the measuring volume. The signal collection is usually arranged at a 90° angle to the direction of the laser beam. At this direction the signal intensity reaches a maximum, and the size of the volume observed can be very well determined. If the vessel or channel enclosing the medium to be investigated allows the installation of a convex mirror opposite to the signal collecting lens, the obtained signal intensity can be remarkably increased. In order to analyse the scattered intensities, the collected light has to be resolved spectrally. This is accomplished either by diffraction units (for example polychromators) or selective filters. The intensity of the light at the selected wavelength is then converted into electronic signals, digitised and then numerically processed.

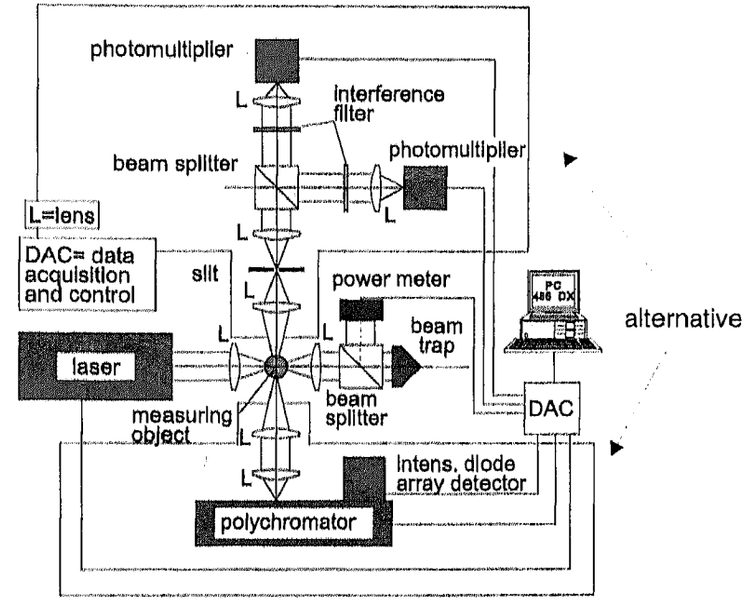

Figure 19. Typical Raman Set-up for point measurements

An example of an investigation with Raman Spectroscopy is shown in Fig. 20. The chemical reaction of a hydrogen flame was analysed there. The experimental set-up was operated under steady-state conditions with a closed tube type burner having a rectangular cross-section. A metal grid was used to stabilise the flame. The pre-mixed unburned gas with a hydrogen concentration of 12 volumetric % approaches the grid upward with a velocity of 17 m/s. There is a separate turbulent flame stabilised behind each opening in the grid, and the burnt gases leave the flame area upward.

The concentration distributions are depicted for each species in the form of levels with various distances from the grid. The first spectrum is taken before the grid; no combustion has taken place up to now, and so there is no steam present. The second spectrum is taken from the main reaction zone. Some of the hydrogen has reacted with parts of the oxygen in the air to form steam as a product. All four species (H_2, O_2, OH, H_2O) and the nitrogen content of the air can be seen in the spectrum. The last spectrum is from a location above the reaction zone, where the under-stoichiometric combustion is complete. Only steam, nitrogen and the surplus oxygen are present there. Assuming the nitrogen behaves like an inert gas - or at least its oxidation is negligible - the temperature can be derived from the change of the integrated area under the nitrogen peak. Of course the temperature of the mixture before the combustion starts has to be known.

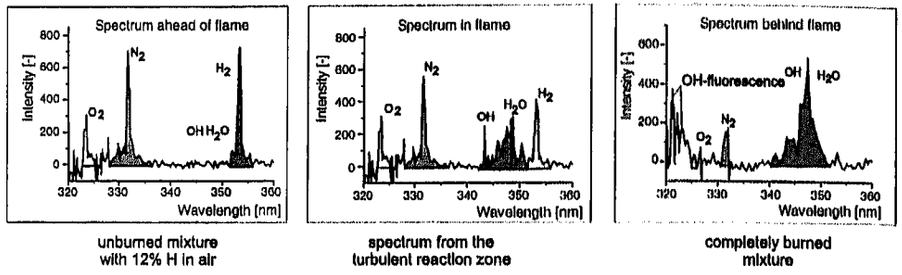

Figure 20. Typical spectra from representative points in a burner: Unburned mixture with 12% H_2 in air
Middle: spectrum from the turbulent reaction zone
Bottom: completely burned mixture

Finally a more practical application of Raman Spectroscopy is presented in Fig. 21, which shows the Raman spectrum of the gas flow in the exhaust pipe of a small motor-bike engine. A lot of unburned hydro-carbons can be detected in this gas flow, which proves that this small piston engine has a low burning efficiency and that it emits toxic gases [16].

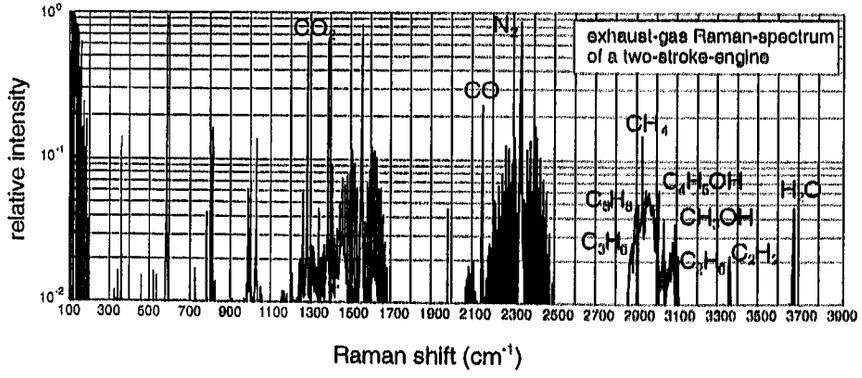

Figure 21. Exhaust-gas Raman Spectrum of a small two-stroke engine (according to Algermissen [16])

4.2 LASER INDUCED FLUORESCENCE

Laser Induced Fluorescence (LIF) and Laser-Induced-Pre-dissociated Fluorescence (LIPF) can be used to measure local concentrations in mass transfer processes or in chemical reactions. A typical arrangement of optical components for performing LIF or LIPF measurements is shown in Fig. 22. A laser beam must be used for the electronic excitation of the molecules of interest. The wave-length of the laser must be adjusted to the substance that is to be investigated. For studying concentration fields in combustion processes, the most active radical of interest in this connection is the OH-radical in hydrogen combustion. The excitation of the OH-radical has to be done with a wave-length of 308 nm and the wave-length of the fluorescing light is of the same value, therefore one has the problem with LIF to distinguish carefully between the primary light of the exciting laser and the secondary light of the OH-fluorescence.

For LIPF-measurements the two wave-lengths are different, for example 248 nm for the exciting light and 290-304 nm for the fluorescing light. Here it is easier to distinguish between primary and secondary light. However, the energy for producing LIPF is much higher than for LIF. To perform LIF for example, an EXCIMER-Laser filled with XeCl can be used, which has a bandwidth of 0,27 nm around the wave-length of 308 nm. To illuminate an area of approximately 50 cm^2 a pulse energy of 150-200 mJ is needed. The pulse duration of EXCIMER-Lasers is around 20 ns.

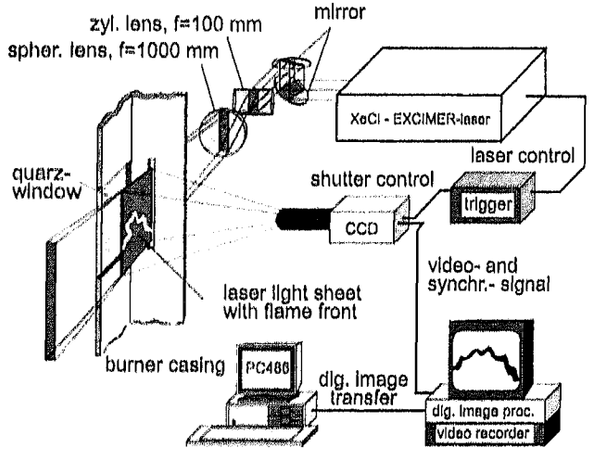

Figure 22. Optical set-up for Laser Induced Fluorescence

Fig. 22 demonstrates how the laser-beam originating from the EXCIMER-Laser is expanded and deformed into a thin light sheet with a height of approximately 5 cm and a thickness less than 0,7 mm. This light sheet travels through a quartz-window into the reaction zone where the fluorescence is produced in this thin layer. The fluorescence is observed and recorded in the perpendicular direction to this light sheet with the aid of a CCD-camera, which is, in this case, intensified in the ultraviolet range. To get a good view of the fluorescing area, large quartz-windows have to be used and the parts, where no optical observations are intended, have to be painted carefully with black colour to

avoid or damp the light scattering in the reaction zone. The video signal of the camera is processed in an image-evaluating unit and transformed into pseudo-colour pictures. These pictures are recorded by a SVHS-video recorder, working in an analogue way. The time-wise coordination of the laser and the camera is done via a triggering unit, which is synchronised by the video-camera.

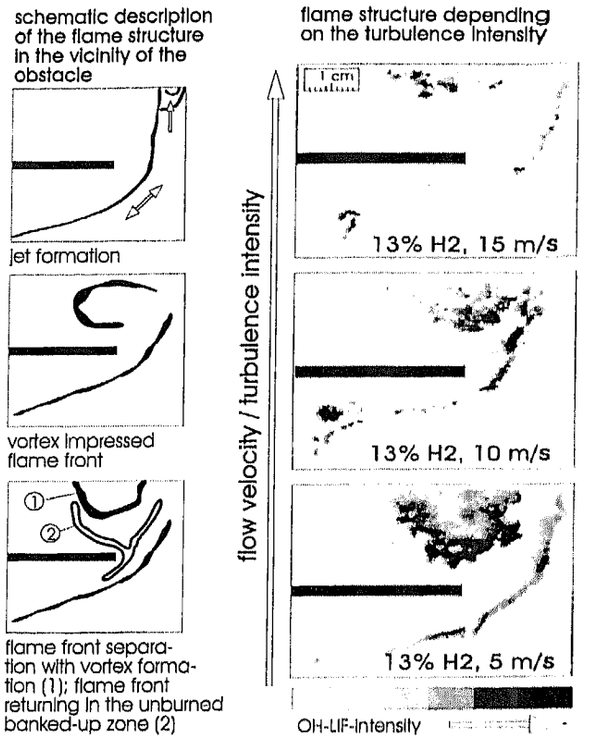

Figure 23. Influence of turbulence on flame formation (H_2-flame)

For LIPF-measurements the same arrangement can be used. However, a laser must be available, emitting light of shorter wave-lengths and higher energy density. This can be done for example by using a Nd-YAG Pump-Dye-Laser or a KrF-EXCIMER-Laser.

This method is very capable, and it is possible to resolve even very thin flame fronts with it. In Fig. 23, the influence of turbulence on the stability of an hydrogen flame is demonstrated [17]. The flame front is travelling in a flowing H_2-air mixture around an obstacle. The obstacle - a rectangular plate - blocked approximately 2/3 of the cross-section of the channel and therefore produced strong turbulence. The H_2-concentration in the air was kept constant at 13% and the flow velocity before the obstacle was varied between 5 and 15 m/s. The laminar flame velocity is the same in all 3 cases of Fig. 23. However, the turbulence changes the true flame velocity remarkably, not only in a positive direction, but it has also the effect of quenching. At low flow velocities we can observe a continuous flamelet passing the area of the obstacle and behind the obstacle a

burning zone, such as in a well stirred reactor. With increasing the flow velocity the flamelet shows more and more gaps of unburned or quenched zones. This is a simple but convincing demonstration that turbulence does not only enhance the combustion; it can also deteriorate it.

4.3 AUTO FLUORESCENCE

Auto Fluorescence can be observed during exothermal chemical reactions. It is based on the fact that some of the radicals or molecules appearing during the chemical reaction already arise in an electronically excited state. A part of these excited radicals radiates energy by spontaneous emission of photons in connection with a change in the energetic state of the molecules which is referred to as chemo-luminescence. The emitted energy is always equal to the difference of the two energetic states involved.

Compared to Laser Induced Fluorescence the Auto Fluorescence has the disadvantage of low spectral signal intensities with the consequence of limited time and special resolution. On the other side, however, it is easy to handle, and it only needs a simple experimental set-up for obtaining insight into the overall structure and behaviour of fast-reacting systems.

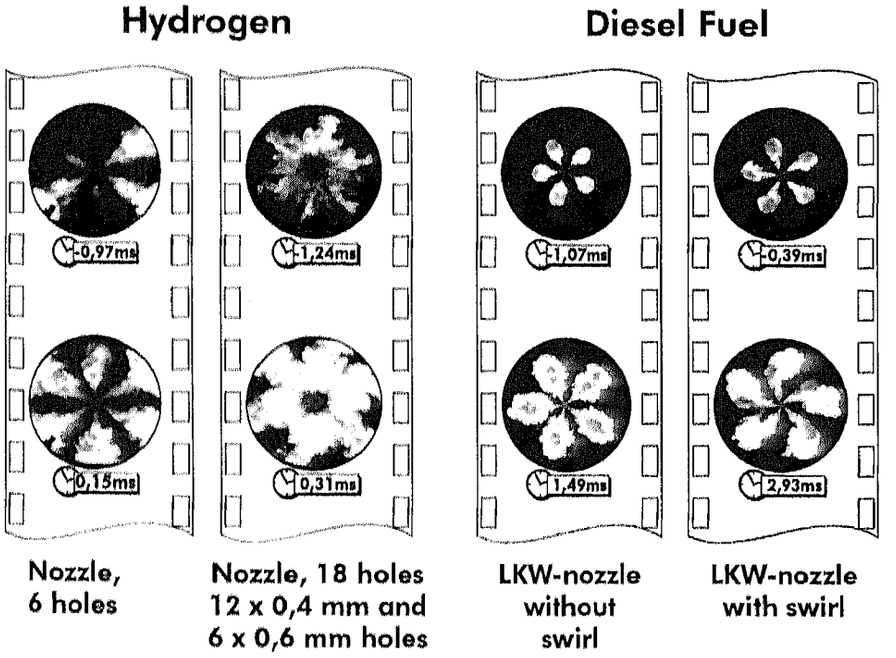

Figure 24. Comparison between the combustion processes of hydrogen and Diesel fuel in a Rapid Compression Machine (The data for the time count from the moment on, when the piston is in the inner dead centre)

An example for a fast-reacting process is the ignition and the combustion in a Diesel-engine in which fuel is injected into a highly compressed air. Due to the compression the temperature of the air is above the ignition temperature of the fuel. This ignition process and the flame propagation is strongly dependent on the injection of the fuel, but also on the properties of the fuel itself. In Fig. 24 examples of such ignition processes and of the flame propagation are presented for 2 different fuels, namely for the usual Diesel-oil and for pure hydrogen. Diesel-oil starts to ignite immediately at the moment when the injection starts and burns smoothly along the injection sprays. If there is a rotating flow in the cylinder, it cannot act at the beginning of the injection onto the flame propagation, because the momentum of the injected spray is too large. After the spray-cloud has expanded, the rotating flow can overcome the radial jet forces and the flame starts to rotate as well.

Hydrogen is much more sensible to the injection mode in spite of the fact, that it is injected in its gaseous phase. There is a big difference in the flame propagation if the same hydrogen amount is injected through 6 holes for example or through 18 holes. In the 6-hole nozzle the hydrogen jets are rather massive and only a few of them start to ignite spontaneously. Only after all 6 jets have been reflected at the cylinder, resulting in an improved mixing, the combustion is well distributed over the circumference. Injecting through 18 holes results in a much better mixing between compressed air and hydrogen from the early beginning, and this affects the combustion process positively. The Auto Fluorescence pictures, shown in Fig. 24, were all photographed through the piston in a specially designed engine, and the time indicated in each picture counts from the moment when the piston reaches the inner dead centre. A negative time indicates a situation before that moment [18].

5. Concluding Remarks

"Computational engineering" is the modern and promising trend not only in research but also in the daily industrial praxis. Without any doubt, modern computers offer very powerful possibilities to predict even complicated thermo-and fluiddynamic processes. We can trust on these predictions only if the physical phenomena are well known so that we can describe them with our "mathematical language". For unknown physical phenomena we have to rely on experiments and here optical measuring techniques provide the very best input for mathematical modelling.

6. References

1. Mayinger, F. (Ed.) (1954) Optical Measurements, Techniques and Applications, *Springer Verlag*, Berlin, Heidelberg.
2. Gabor, D. (1948) A New Microscopic Principle, *Nature* 161; (1949) Microscopy by Reconstructed Wavefronts, *Proc. Roy. Soc.* A 197; (1951) Microscopy by Reconstructed Wavefronts II, *Proc. Roy. Soc.* A 197.
3. Caulfield, H.J.; Sun Li (1970) The Applications of Holography, *Wiley*, New York.
4. Collier, C.B.; Burckhardt; Sun Li (1971) Optical Holography, *Academic Press*, New York.
5. Smith, H.M. (1977) Holographic Recording Materials, *Springer Verlag*, Berlin, Heidelberg, New York.
6. Gebhard, P.; Mayinger, F. (1996) Evaluation of Pulsed Laser Holograms of Flashing Sprays by Digital Image Processing, Flow Visualisation and Image Processing of Multiphase Systems, *ASME*, FED-Vol. 209.
7. Gebhard, P. (1996) Zerfall und Verdampfung von Einspritzstrahlen aus lamellenbildenden Düsen, *Dissertation*, Technische Universität München.
8. Feldmann, O.; et al. (1997) Evaluation of Pulsed Laser Holograms of Flashing Sprays by Digital Image Processing and Holographic Particle Image Velocimetry, *Proc., CSNI Specialist Meeting on Advanced Instrumentation*, Santa Barbara, USA.
9. Panknin, W.; Mayinger, F. (1974) Holography in Heat and Mass Transfer, *5th Int. Heat Transfer Conference*, Tokio, VI 28.
10. Panknin, W. (1977) Eine holographische Zweiwellenlängen Interferometrie zur Messung überlagerter Temperatur- und Konzentrationsgrenzschichten, *Dissertation*, Universität Hannover.
11. Nordmann, D.; Mayinger, F. (1981) Temperatur, Druck und Wärmetransport in der Umgebung kondensierender Blasen, *VDI-Forschungsheft* 605.
12. Bohren, C.F.; Huffmann D.R. (1983) Absorption and scattering by small particles, *John Wiley and Sons*, New York.
13. Long, D.A. (1977) Raman spectroscopy, *Mc Graw-Hill*, London.
14. Alonso, M.; Finn, E.J. (1988) Quantum Physics, *Addison-Wesley*.
15. Hanson, R.K.; Seitzmann, J.M.; Paul, P.H. (1990) Planar fluorescence imaging of combustion gases, *Applied Physics*, Vol. B 50.
16. Algermissen, Personal communication, University Stuttgart.
17. Ardey, N; Mayinger, F. (1995) Influence of transport phenomena on the structure of lean premixed hydrogen air flames, *11th Proc. Of Nuclear Thermal Hydraulics*, San Francisco, California, Oct. 29 – Nov. 2 and *Amer. Nuclear Soc.*, S. 33-41 (ANS Order No. 700227).
18. Dorer, F.; Prechtl, P.; Mayinger, F. (1997) Investigation of mixture formation on combustion processes in a hydrogen fuelled Diesel engine, *HYPOTHESIS II, Intern. Symposium*, Aug. 18-22, Grimstadt, Norway (to be published).